



Provenance studies of southern Tanzania river sediments: Heavy mineral signatures and U–Pb zircon ages



Katrine Fossum^{a,*}, Henning Dypvik^a, Andrew Morton^b

^a University of Oslo, Department of Geosciences, Boks 1047 Blindern, 0316, Oslo, Norway

^b Giddanmu, Musselwick Road, St. Ishmaels, Pembrokeshire, SA62 3TJ, United Kingdom

ARTICLE INFO

Keywords:

Sedimentary provenance
River sediments
Coastal Tanzania
Source-to-sink
U/Pb zircon ages
Heavy mineral analysis

ABSTRACT

Detrital zircon U–Pb geochronology and heavy mineral data from four main rivers in coastal southern Tanzania - the Rufiji, Matandu, Mbwemkuru and Ruvuma rivers - are compared with the bedrock geology of their catchment and with data from the Mesozoic strata of the Mandawa Basin, also in coastal Tanzania. The objective is to evaluate the source-to-sink pattern of sedimentation through time, between the Mesozoic and present day.

The recent river sediments display variations in both heavy mineral assemblages and U–Pb zircon populations, reflecting their different catchment areas. The Matandu and Mbwemkuru rivers transport sediments characterised by amphibole-dominated heavy mineral assemblages, whereas the great Rufiji and Ruvuma rivers are characterised by more stable heavy mineral assemblages. The detrital zircon populations show age peaks at c. 2900–2500, 2000–1800, 1000, 800 and 700–500 Ma, the common denominators are the Late Mesoproterozoic (c. 1000 Ma) and Late Neoproterozoic (700–500 Ma) age fractions. The Rufiji River and the Matandu River display similar zircon age distributions, both containing abundant Palaeoproterozoic zircons, interpreted as recycled from Karoo successions in a part of the Selous Basin which is drained by both rivers. The Mbwemkuru and Ruvuma rivers contain mainly Late Mesoproterozoic and Late Neoproterozoic aged zircons that were supplied from the Unango and Marrupa complexes and the Cabo Delgado Nappe Complex/Eastern Granulites. The more diverse zircon population in the Rufiji and Matandu river is likely reflects recycling of older sedimentary successions in addition to sediments supplied from basement lithologies.

1. Introduction

Provenance evaluation of fluvial sediments allows us to indirectly examine erosion and sediment generation in the hinterland, by comparing the results with data from the rock record of the palaeo-drainage system (Alizai et al., 2011). Actualistic studies of fluvial sediments allow for more precise provenance interpretations of older sedimentary sequences, because the bedrock geology of the catchments is in many cases well known. The provenance of modern river sediments may consequently be used to discriminate and identify sediment sources of the past, and to study changes in the hinterland.

We have investigated heavy mineral assemblages and isotopic U–Pb zircon ages in sand from four major rivers along the southern coast of Tanzania: the Rufiji River, the Matandu River, the Mbwemkuru River and the Ruvuma River (Fig. 1). The perennial Rufiji and Ruvuma rivers have very large catchment basins: the Rufiji River Basin in the north and the Ruvuma River Basin in the south. The two smaller and seasonal rivers, the Matandu River and the Mbwemkuru River, are located

between the Rufiji and Ruvuma, and flow through the Mesozoic Mandawa Basin before entering the Indian Ocean (Fig. 1). The purpose of the study presented here is to evaluate the provenance of the fluvial sediments from each of these four rivers and to compare the results with published provenance studies of Mesozoic and Cenozoic successions in the Mandawa Basin (Fig. 1) where similar analytical approaches have been applied.

The composition of fluvial sediments delivered into the ocean is governed by the size and geology of the catchment area, relief and topography, climate and weathering, mineral sorting and alteration during transportation, and the mechanical and chemical stability of the minerals. Alluvially stored sediments, e.g. on floodplains or dried out river beds, are susceptible to weathering and leaching (Morton and Hallsworth, 1994). If the catchment also comprises sedimentary formations, the heavy minerals derived from those rocks will dilute the provenance signature with components reflecting an ancient source-to-sink system. Rivers draining different geochronological terranes should be expected to give polymodal zircon age-distributions determined by

* Corresponding author.

E-mail address: fossum.katrine@gmail.com (K. Fossum).

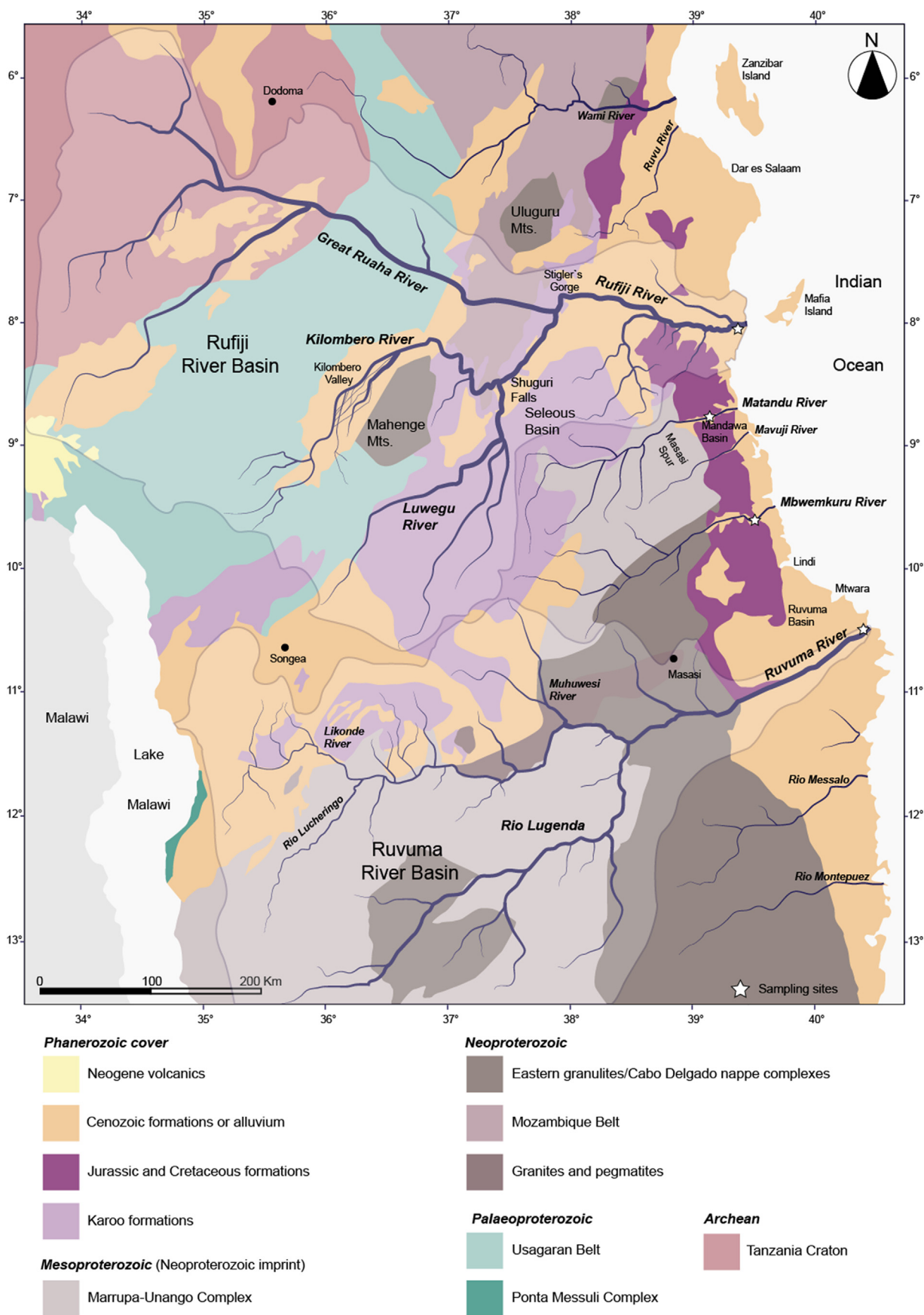


Fig. 1. Geological map of south-central Tanzania and northern Mozambique and the main rivers of the area. The extents of the Rufiji and Ruvuma river catchments have been marked on the map. Map compiled from Pinna et al. (2004), Bingen et al. (2009), Sommer et al. (2017)) and Mtabazi et al. (2019).

the relative size, rates of erosion and zircon fertility of the catchments (Malusa et al., 2016). Because zircon is a highly resistant mineral to both physical and chemical alteration it can survive several erosion-transport-deposition cycles, homogenising material from various proto-sources over long periods of time (Andersen et al., 2016). These recycled zircons will reflect the source of the sandstones, and hence preserve the memory of an ancient source-to-sink system. This is an important limitation for using detrital zircon geochronology in provenance studies because identifying recycled grains is in most cases not possible.

1.1. Bedrock geology of the river catchments

The river catchments comprise various geological terranes, ranging in age from Archean to Recent sediment cover sequences. The central part of Tanzania is occupied by the Archean Tanzania Craton which is surrounded by remnants of Proterozoic mobile belts (Figs. 1 and 2) that were later subjected to several Phanerozoic rifting events.

The Palaeoproterozoic Usagaran Belt (Fig. 1) defines an orogenic phase that lasted from 2000 to 1800 Ma in which portions of Archean craton were reworked (Fritz et al., 2005). The Usagaran Belt (Fig. 1) is composed of medium to high-grade metamorphic rocks that are products of oceanic subduction followed by deformation and magmatism in a volcanic arc setting (Fritz et al., 2005; Boniface and Schenk, 2012).

The Mesoproterozoic Irumidian Orogeny occurred during the assembly of Rodinia and involved crustal reworking of the Archean Congo-Tanzania Craton (Fig. 2). The resulting Irumide Belt is a NE-trending fault and thrust belt that stretches from central Zambia to the Zambia-Tanzania-Malawi border (De Waele et al., 2006). The Unango and Marrupa complexes are mainly felsic orthogneisses that were emplaced between c. 1062 and 946 Ma, and metamorphosed to amphibolite – granulite facies at c. 953 Ma (Bingen et al., 2009). In southern Tanzania, Mesoproterozoic orthogneisses with protolith ages of 1056–956 Ma are interpreted as the continuation of the Unango and Marrupa complexes into SE Tanzania (Kröner et al., 2003; Hauzenberger et al., 2014; Mtabazi et al., 2019).

The Unango and Marrupa complexes were affected by the later Kuunga Orogeny. Post-collisional felsic plutons dated at 549 ± 13 and 486 ± 27 Ma have been reported from the Unango Complex (Bingen et al., 2009).

Shortly after Rodinia broke up (870–800 Ma), Gondwana started to assemble (c. 800 to 500 Ma) (Torsvik and Cocks, 2013). Two major orogenic cycles in relation to Gondwana assembly have been recognised in the study area (Fig. 3): the N–S trending East African Orogeny (760–600 Ma) and the E–W trending Kuunga Orogeny (600–500 Ma) (Meert, 2003; Fritz et al., 2013; Mtabazi et al., 2019). The N–S trending Mozambique Belt (Figs. 1 and 3) is a section of the East African Orogen in Tanzania and Mozambique; it hosts both juvenile rocks and reworked Archean and Palaeoproterozoic rocks (Fritz et al., 2005). The Mozambique Belt is bounded to the west by the Usagaran Belt in Tanzania, and in Mozambique by the Unango and Marrupa complexes (Fig. 1). In Tanzania the Mozambique Belt can be divided into two lithotectonic units: the Eastern Granulites and the Western Granulites (Fritz et al., 2005). The Western Granulites form the lower structural unit of the Mozambique Belt, composed of reworked Archean and Palaeoproterozoic crusts metamorphosed during the East African Orogeny (Fritz et al., 2005). The Eastern Granulites form the upper tectonic unit of the Mozambique Belt and are juvenile rocks emplaced between 900 and 700 Ma and overlain by a metasedimentary suite metamorphosed during the East African Orogeny (600–620 Ma). Zircons from anorthosite in the Uluguru and Mahange mountains have yielded U–Pb ages of 880 to 820 Ma and 800 to 739 Ma, respectively (Tenczer et al., 2006). The Eastern Granulites continue southwards into Mozambique as the Cabo Delgado Nappe Complex, Fig. 1 (Pinna et al., 1993; Fritz et al., 2013). The Cabo Delgado Nappe Complex is genetically similar to the Eastern Granulites in Tanzania; both are composed of mafic

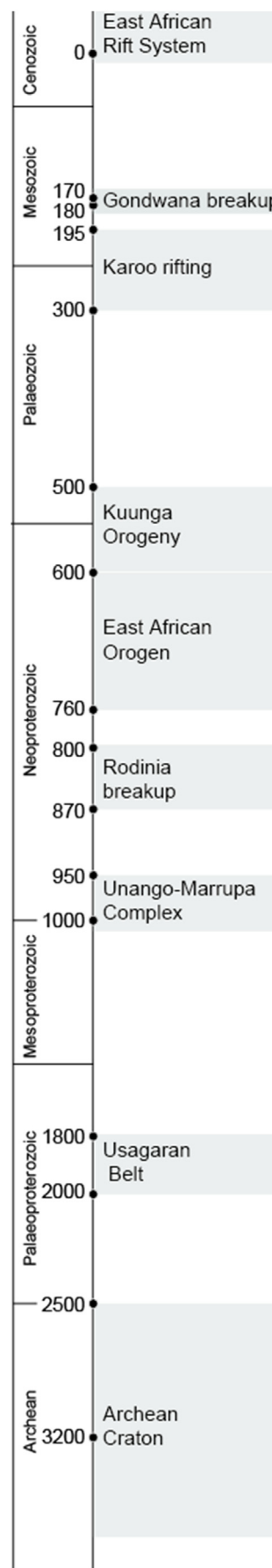


Fig. 2. Timeline of the main tectonic events of the study area.

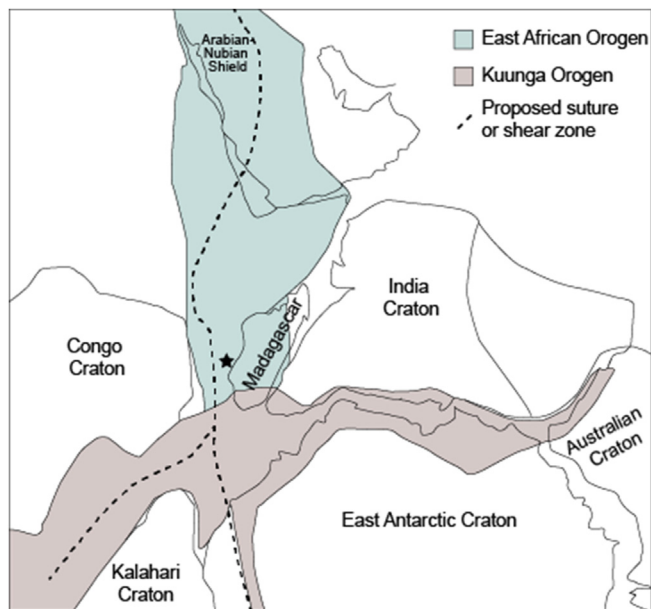


Fig. 3. Eastern Gondwana after the Neoproterozoic amalgamation of Gondwana, showing the extent of the N–S trending East African Orogeny (760–600 Ma), and the E–W trending Kuunga Orogeny (600–500 Ma). The approximate position of the Mandawa Basin is marked with a star. Modified from Meert (2003).

granulites, volcanic arc lithologies and supracrustal rocks. Peak metamorphism in the Cabo Delgado Nappe Complex has been dated to c. 555 Ma (Bingen et al., 2009).

SE Tanzania and N Mozambique are positioned at the intersection between the Mesoproterozoic Unango and Marrupa complexes and two Late Neoproterozoic belts, giving rise to the complex geology in this area. In the Late Neoproterozoic the study area was located in a transition zone between the N–S trending East African Orogeny and the E–W trending Kuungan Orogeny (Fig. 2) (Mtabazi et al., 2019). The relationships between the Meso- and Neoproterozoic suites are not well understood in Tanzania because these lithotectonic units are partly covered by Phanerozoic rift basins e.g. the Selous, Mandawa and Ruvuma basins, and recent sedimentary cover sequences (Mtabazi et al., 2019). The Jurassic Mandawa Basin is separated from the Permo–Triassic Selous Basin by a basement complex called the Masasi Spur (Fig. 1) that comprises different lithotectonic units: the Neoproterozoic Eastern Granulites/Cabo Delgado Nappe Complex and the Mesoproterozoic Unango and Marrupa complexes (Kröner et al., 2003; Mtabazi et al., 2019).

Several episodes of rifting occurred during the Phanerozoic, e.g. Karoo rifting, rifting resulting in the Early Jurassic breakup of Gondwana, and the ongoing rifting associated with the southward propagation of the East African Rift System, Fig. 2 (Mbede, 1991). Much of south-central Tanzania is occupied by sedimentary basins (Fig. 1). Presently, the Rufiji River Basin drains several of these sedimentary basins, and they must be evaluated as potential sources for the sediments that are transported into the Indian Ocean by the Rufiji River today, and most likely also in the past.

The term Karoo is applied to successions deposited during a widespread Gondwanian sedimentation cycle from Late Carboniferous to Early Jurassic, representing a first-order supercontinent cycle: the assembly and break-up of Pangea (Catuneanu et al., 2005). The intracratonic Karoo basins of Tanzania generally trend NNE–SSW (Kent et al., 1971; Mpanda, 1997; Nicholas et al., 2007), and comprise upwards-fining megacycles (alluvial, fluvial, deltaic and lacustrine) initiated by periodic faulting (Mbede and Dualeh, 1997; Wopfner, 2002), peaking in the Middle Permian (Macgregor, 2017). Another major

rifting period occurred later in the Triassic, strongly affecting mainly the coastal strip stretching from Somalia to Tanzania, and western Madagascar (Macgregor, 2017).

A new phase of rifting commenced in the Early Jurassic that would lead to the breakup of Gondwana (Geiger et al., 2004; Gaina et al., 2013; Reeves, 2018; Tuck-Martin et al., 2018). Extension occurred in a NW–SE direction and created a seaway which propagated southwards from the Tethys Ocean in the north. Early marine incursions flooded depressions along the coastal margins of Somalia, Kenya, Tanzania (Mandawa Basin) and western Madagascar, and evaporites accumulated locally in restricted basins (Rabinowitz et al., 1982). At around 170 Ma, Gondwana split roughly parallel to the modern East African Margin to form West Gondwana (Africa and South America) and East Gondwana (Madagascar, India, Antarctica and Australia) (Geiger et al., 2004; Gaina et al., 2013; Reeves, 2018), and seafloor spreading commenced shortly after (Eagles and König, 2008; Gaina et al., 2013; Tuck-Martin et al., 2018). After breakup, fault activities diminished and the margin segments started to subside, marking the onset of the first major transgression forming an epeiric sea between the conjugate East African - Western Madagascan margins.

Fission track analysis of basement rocks in Tanzania found that increased erosion and denudation occurred during the Mesozoic; in the Triassic (250–200 Ma), Middle Jurassic, Late Jurassic and Early Cretaceous (140–120 Ma) (Noble and Foster, 1997; Van der Beek et al., 1998; Said et al., 2015).

1.2. River information

The rivers from which the sands were sampled flow roughly from W to E, crossing the hot and humid coastal lowland before entering the Indian Ocean. The Matandu and Mbemkuru rivers are small relative to the Rufiji and Ruvuma rivers. The Rufiji and Ruvuma have developed large river-mouth deltas each extending over more than 1400 km² (Bourget et al., 2008).

The Rufiji River Basin (Fig. 1) is the largest river basin in Tanzania and drains most of southeastern Tanzania, approximately 180,000 km² (Bourget et al., 2008). The Rufiji River Basin is composed of three sub-basins, Fig. 1: the Kilombero, the Great Ruaha and the Luwegu, and the catchment is comprised of different types of bedrock (Archean Craton, Usagaran Belt, Mozambique Belt, sedimentary basins and alluvium), vegetation, relief and climatic conditions (Temple and Sundborg, 1972). The Rufiji River proper starts at the Shuguri falls where the Luwegu and the Kilombero rivers meet and is joined by the Great Ruaha some 193 km from the Indian Ocean (Fig. 1). The Great Ruaha River (Fig. 1) drains almost half of the Rufiji River Basin but accounts for only 13% of the average total discharge from the Rufiji Basin. The low discharge is explained by most of the catchment being located on the dry highland plateau where the yearly precipitation is low and seasonally fluctuating (Temple and Sundborg, 1972). The headwaters of the Great Ruaha River are located on the Archean Craton to the west and flow eastwards through the Palaeoproterozoic Usagaran Belt and the Neoproterozoic Mozambique Belt, crossing several Karoo and Mesozoic sedimentary basins and alluvial deposits (Fig. 1). The Great Ruaha River joins the Rufiji just upstream of Stiegler's Gorge (Fig. 1) before entering the Rufiji River floodplain some 160 km from the ocean (Temple and Sundborg, 1972). The Luwegu River drains the south-eastern part of the Rufiji River Basin. Its catchment covers about 18% of the Rufiji River Basin (Fig. 1) and contributes approximately one fifth of the total discharge into the Indian Ocean (Temple and Sundborg, 1972). The Luwegu follows Karoo lineaments and drains most of the Selous Basin where the bedrock is mainly Karoo rocks (Haldemann, 1962; Hankel, 1987). The Kilombero River is the main tributary to the Rufiji River: it drains just one fifth of the Rufiji River Basin but accounts for over half of the discharge from the Rufiji River Basin. The headwaters drain a small part of the Usagaran Belt before entering the Kilombero Valley floodplains. The Kilombero River joins the Luwegu at Shuguri

falls (Fig. 1), an area underlain by Karoo rocks (Haldemann, 1962; Temple and Sundborg, 1972).

The Ruvuma Basin catchment (Fig. 1) is slightly smaller than the Rufiji Basin, covering 163,500 km² (Bourget et al., 2008). The Ruvuma River straddles the Mozambique – Tanzania boundary, and drains the southernmost part of Tanzania and northern Mozambique (Fig. 1). Most of the catchment area lies in Mozambique, the Tanzanian tributaries and their catchments being generally small (Fig. 1). The main Ruvuma Basin tributary is the Rio Lugenda which lies entirely in Mozambique and drains the Cabo Delgado Nappe and the Unango and Marrupa complexes. The Tanzanian tributaries drain similar lithologies in addition to sedimentary formations (Fig. 1).

The area between the Rufiji and Ruvuma rivers is occupied by smaller rivers, draining the areas to the west, outside of the Rufiji and Ruvuma river basins. The Matandu and Mbwemkuru rivers are the two largest rivers flowing through the Mesozoic Mandawa Basin (Fig. 1). Most of their catchments are in the Masasi Spur to the west of the Mandawa Basin (Fig. 1). The Matandu River rises in the Selous Basin (Fig. 1) and drains a minor portion of the Karoo rocks exposed there (Hankel, 1987).

2. Materials and methods

Single sediment samples of fine to medium grained sand were collected from each of the four rivers in the coastal lowland. The sediment sampled from the Rufiji River and the Ruvuma River was collected closer to the river outlets to the Indian Ocean, whereas the Mbwemkuru River and Matandu River samples were collected in dried up river valleys a few kilometres inland (Fig. 1). Consequently, the Rufiji and Ruvuma sediment samples may have experienced more hydraulic sorting than the samples from the Mbwemkuru and Matandu rivers.

2.1. Conventional heavy mineral analysis

In this study we have analysed the non-opaque heavy mineral assemblage from the 63–125 µm fraction of the sampled river sediments. The heavy minerals were separated from the light minerals using bromoform heavy liquid (2.8 gm/cc) and identified using optical microscopy. The heavy mineral assemblage was determined by counting and classifying 200 non-opaque grains for each sample.

A separate count was done to calculate the provenance-sensitive index values apatite to tourmaline (AT), garnet to zircon (GZi), rutile to zircon (RuZi), and monazite to zircon (MZi). These index values were determined on the basis of separate counts for each mineral pair, e.g. the ATi (index) was calculated using 100 x apatite count/(total apatite + tourmaline) following the procedure of Morton and Hallsworth

(1994). Some rare minerals not observed during the 200 grain count but noted during the calculation of the provenance-sensitive index ratios are denoted as “R” in the results table and present in abundances less than 0.5%.

2.2. Detrital zircon U–Pb analysis

Zircons were randomly picked from the heavy mineral separates (63–125 µm), mounted in epoxy, and polished. U–Pb analysis was done by laser ablation inductively coupled plasma mass spectrometry (LA-ICP-MS) at the Department of Geosciences, University of Oslo. A Nu Plasma HR-multi collector mass spectrometer equipped with a Cetac LSX-213 G2+ laser microprobe was used on four samples. The analytical protocols G2+ of Andersen et al. (2009) were followed.

Data reduction was done using an interactive, in-house Microsoft Excel 2003 spreadsheet. U–Pb standards used during analysis were: GJ-1 (Belousova et al., 2006), 91500 (Wiedenbeck et al., 1995), and A382 (Huhma et al., 2012). Grains with more than ± 10% discordance were discarded. For an analysis with $^{207}\text{Pb}/^{235}\text{U} = x$, $^{206}\text{Pb}/^{238}\text{U} = y$ and $^{207}\text{Pb}/^{206}\text{Pb} = t$, the central discordance (%) was calculated using the equation:

$$\text{disc} = 100 \left(\sqrt{\frac{x^2 + y^2}{(e^{\lambda_{235}t} - 1)^2 + (e^{\lambda_{238}t} - 1)^2}} - 1 \right)$$

where λ_{235} and λ_{238} are the decay constants of ^{235}U and ^{238}U , respectively (Steiger and Jäger, 1977). The $^{206}\text{Pb}/^{238}\text{U}$ ages were used if younger than or equal to 600 Ma, and $^{207}\text{Pb}/^{206}\text{Pb}$ ages if older than 600 Ma.

The U–Pb results obtained by the LA-ICP-MS were processed using the open access *detzrcr* version 0.2.5 software package, available at <https://CRAN.R-project.org/package=detzrcr> (Andersen et al., 2018). Kernel density estimate curves and the empirical cumulative distribution functions (ECDF) were constructed for each of the samples. The Kernel density estimate curves visualise the age frequency distributions in a sample but do not explicitly consider the uncertainty in distribution patterns caused by the sampling process. Therefore, the age distribution patterns were plotted in cumulative distribution curves with 95% confidence bands to assess differences/similarities within data sets (Andersen et al., 2018).

3. Results

3.1. Conventional heavy mineral analysis

The four river sediment samples display variations in their heavy mineral assemblages (Fig. 4, Table 1) and consequently in their

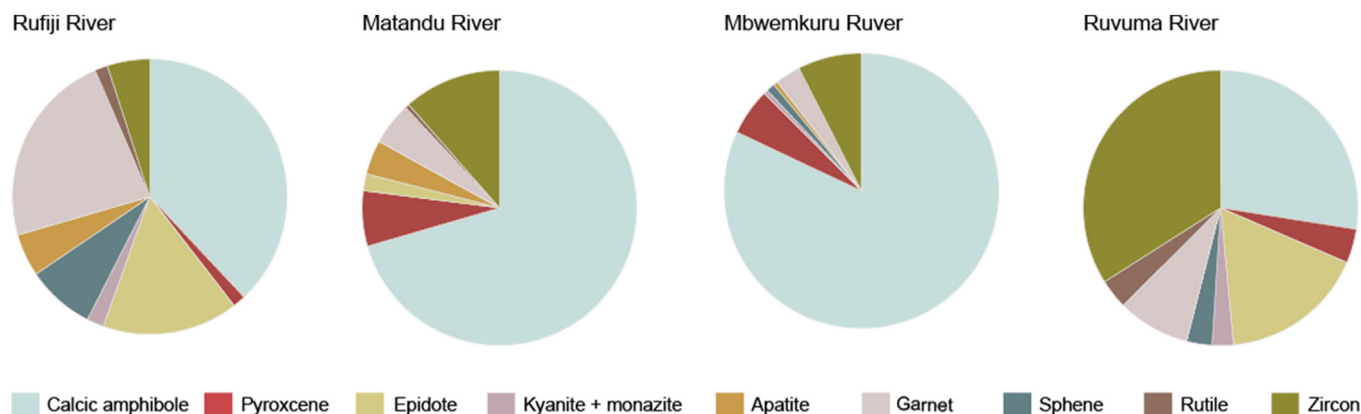


Fig. 4. The non-opaque heavy mineral assemblages from the analysed river sediments illustrated as pie charts. The Matandu and Mbwemkuru river separates are characterised by high amounts of unstable minerals (calcic amphibole and pyroxene) and less diverse heavy mineral assemblage relative to the Rufiji and Ruvuma river sediment samples.

Table 1Relative abundance of non-opaque detrital heavy minerals in the 63–125 μm fraction (expressed as frequency %).

Sample	UTM	At	Ap	Ca	Cp	Ep	Gh	Gt	Ky	Mo	Op	Ru	Sa	Sl	Sp	St	To	Zr
Rufiji	0496797, 9113543		5.	38	1	16		23	2	R	0.5	1.5		R	8	R	R	5
Matandu	0488811, 9026855	R	4.	70.5	4	2		5		R	2.5	0.5			R			11.5
Mbwemkuru	0507790, 8929900		0.5	82.	4			3		0.5	1.5	R			1		R	7.5
Ruvuma	0651105, 8836863		R	27.5	1	17	R	8.5		2.5	3	3.5	R		3	R	R	34

At - anatase, Ap - apatite, Ca - calcic amphibole, Cp - clinopyroxene, Ep - epidote, Gh - gahnite, Gt - garnet, Ky - kyanite, Mo - monazite, Op - orthopyroxene, Ru - rutile, Sa - sodic amphibole, Sl - sillimanite, Sp - titanite, St - staurolite, To - tourmaline, Zr - zircon. R - rare (< 0.5%).

Table 2

The provenance-sensitive index ratio values determined from the heavy mineral separates.

Sample	ATi	total	GZi	total	RuZi	total	MZi	total
Rufiji	91	100	79.4	252	15.3	118	5.7	106
Matandu	100	100	25.5	200	6.1	213	5.2	211
Mbwemkuru	98	50	35	200	3	197	7.7	207
Ruvuma	95.8	24	25	200	10.7	224	2.9	206

ATi - Apatite-Tourmaline index, GZi - Garnet-Zircon index, RuZi - Rutile-Zircon index, MZi - Monazite-Zircon index.

provenance-sensitive index values (Table 2). The Matandu and Mbwemkuru rivers display very similar heavy mineral assemblages, and differ from the Rufiji and Ruvuma separates by having a higher content of unstable heavy minerals (amphibole and pyroxene). The heavy mineral assemblages from the Rufiji and Ruvuma river separates are different from each other, and from the heavy mineral assemblages of the Matandu and Mbwemkuru rivers (Fig. 4, Table 1).

3.1.1. Rufiji River

The Rufiji River sample shows a diverse heavy mineral assemblage composed of calcic amphibole, garnet, epidote, sphene, zircon and apatite, with minor amounts of typical metamorphic minerals (clinopyroxene, kyanite, monazite, rutile and orthopyroxene) (Fig. 4, Table 1). The sediments from the Rufiji River are the most garnetiferous of the samples analysed, which is reflected in the high GZi value of 79.4 (Table 2). The RuZi value is also the highest of the four samples analysed.

3.1.2. Matandu and Mbwemkuru River

The Matandu and Mbwemkuru river sediments contain less diverse and less stable heavy mineral assemblages than the Rufiji River and Ruvuma River samples. Their separates are characterised by high contents of calcic amphibole, 70.5 and 82% respectively (Fig. 4). Pyroxene, another unstable heavy mineral, constitutes 6.5% in the Matandu river sample and 5.5% in the Mbwemkuru river sample (Table 1). Garnets account for 5% of the heavy mineral assemblage in the Matandu river separate and 3% in the Mbwemkuru river separate, resulting in low GZi values of 25.5 and 35.0 respectively (Table 2). Zircon is the second most abundant mineral, with 11.5% in the Matandu sample and 7.5% in the Mbwemkuru sample. High zircon and low rutile contents give low RuZi values (Table 2). Epidote is rare in the Matandu River separates (2%) and absent in the Mbwemkuru sample (Table 1).

3.1.3. Ruvuma River

The heavy mineral separates from the Ruvuma River are characterised by high content of zircon (34%) and low amounts of calcic amphibole (27.5%) compared to the three rivers to the north (Fig. 4, Table 1). Epidote is common and constitutes 17% of the total non-opaque heavy mineral fraction. The low GZi value of 25 reflects the low amounts of garnet and high amounts of zircon in the sample (Tables 1 and 2).

3.2. U–Pb zircon ages

The U–Pb zircon ages of the riverine sediments display variations from sample to sample. The detrital zircons can be grouped into five main age populations: c. 2900–2500, 2000–1800, 1000, 800, 700–500 Ma. The common denominators in all samples are the Late Mesoproterozoic to Early Neoproterozoic (1087–935Ma), and Late Neoproterozoic (610–489 Ma) age fractions (Fig. 5). Palaeoproterozoic grains (2068–1747 Ma) are abundant in the Rufiji and Matandu river samples.

The empirical cumulative distribution curves, Fig. 6, show that the zircon populations in the Rufiji and the Matandu samples display fairly similar age fractions, but that this pair of curves is very different from the pair of curves for the Ruvuma and Mbwemkuru river samples which show that these two rivers share similar zircon populations.

3.2.1. Rufiji River

Of 98 zircon analyses, 63 were < 10% discordant (Fig. 5). Two thirds of the zircon population in the Rufiji River sample comprises equal amounts of Palaeoproterozoic (2068 ± 10 to 1849 ± 12 Ma) and Late Mesoproterozoic to Early Neoproterozoic (1058 ± 11 to 891 ± 12 Ma) zircons. The Rufiji sample also has a noticeable content of Late Neoproterozoic – Cambrian grains (610 ± 9 to 493 ± 10 Ma). A few Archean grains and a single 1300 Ma grain were also identified.

3.2.2. Matandu River

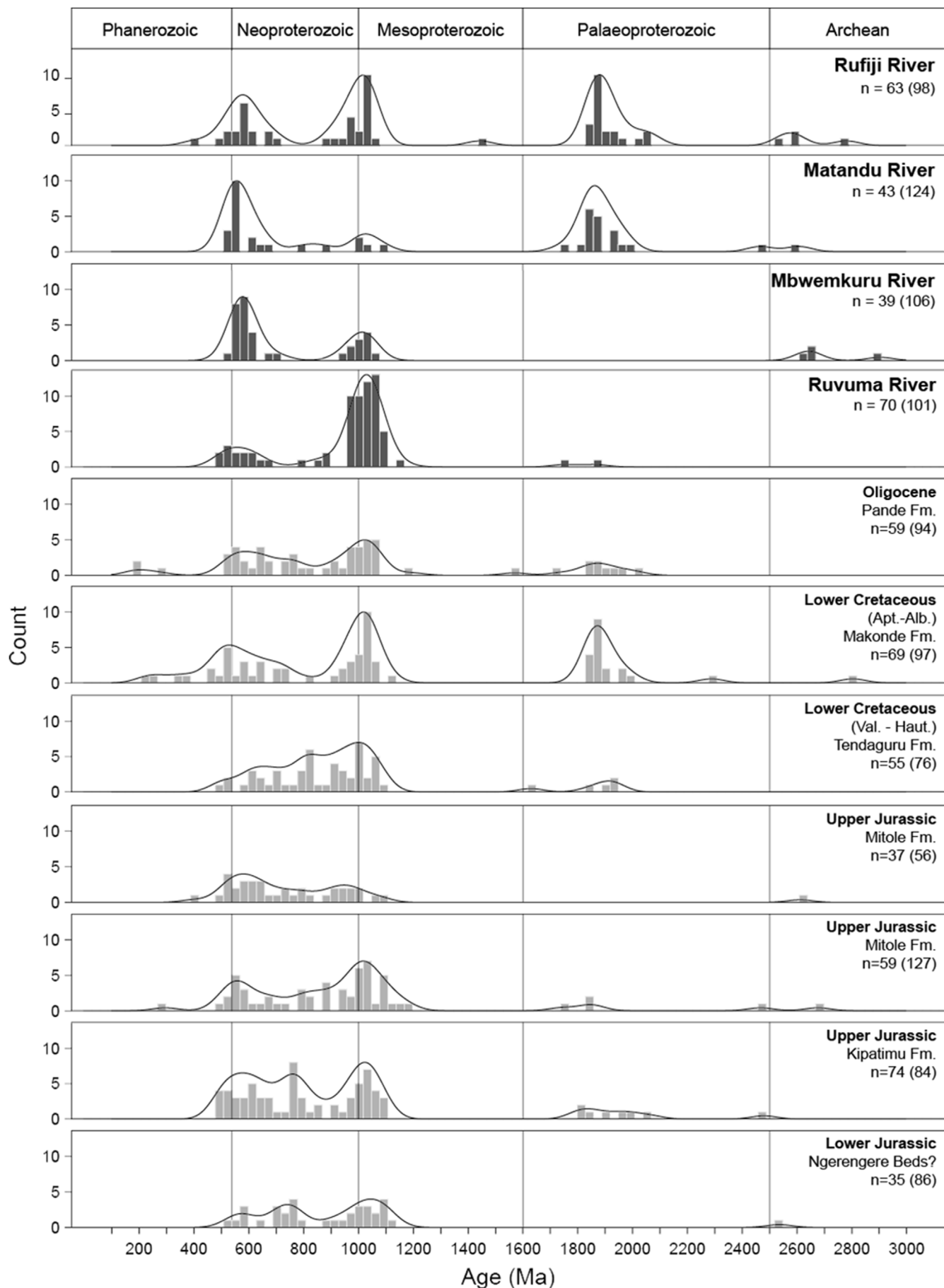
Of 124 zircon analyses, 43 were < 10% discordant (Fig. 5). The Matandu River sample has the highest content of Palaeoproterozoic zircons (1958 ± 27 to 1747 ± 26 Ma) of all the analysed samples. There is also a noticeable population of Late Neoproterozoic – Cambrian grains (702 ± 19 Ma to 536 ± 11). A few grains gave Late Mesoproterozoic to Early Neoproterozoic (between 1100 and 800 Ma) and Archean ages.

3.2.3. Mbwemkuru River

Of 106 zircon analyses, 39 were < 10% discordant (Fig. 5). Characteristic for the Mbwemkuru River sample is the absence of Palaeoproterozoic grains. Just over half of the concordant zircons group within the time window of the Kuunga Orogeny (527 ± 6 to 608 ± 14 Ma), and ten percent show East African Orogen (EAO) ages. Late Mesoproterozoic to Early Neoproterozoic (935 ± 6 to 1056 ± 23 Ma) zircons are also common. A few Archean grains were detected.

3.2.4. Ruvuma River

Of 101 zircon analyses, 70 were < 10% discordant (Fig. 5). Two thirds of the concordant zircons in the Ruvuma River sample group in the Late Mesoproterozoic to Early Neoproterozoic age fraction (969 ± 10 to 1059 ± 9 Ma). Except for two Palaeoproterozoic grains, the remaining grains are Neoproterozoic.



(caption on next page)

Fig. 5. The U/Pb results for river sediment and Mandawa Basin sandstones plotted in Kernel density estimate curves (KDE) for the using 48 Ma bandwidth, and 30 Ma binwidth. n = concordant grains, numbers in brackets = grains analysed.

4. Discussion

4.1. Provenance evaluation based on the heavy mineral data and U–Pb zircon ages

Both the heavy mineral and zircon data show variations in the analysed sediment composition, possibly a result of drainage of different source terranes and local variations in weathering. However, assessing the sediment provenance by only using conventional heavy mineral analysis is difficult because different source terranes can supply the same minerals or similar mineral groups. Nonetheless, it is a practical and simple method to detect compositional variations in the heavy mineral assemblage as a result of different sediment provenance between samples/formations.

Separates from both the Rufiji and Ruvuma rivers contain less of the more unstable heavy minerals (amphiboles and pyroxenes) compared to sands of the smaller rivers (Table 1). In the larger catchment areas of the Rufiji and Ruvuma river basins unstable minerals have greater potential to be lost during transport and/or temporal sediment storage in the river systems. In the Ruvuma River sample, two thirds of the non-opaque heavy mineral fraction are zircons, possibly a result of hydraulic sorting during transport and deposition.

The catchments of the Matandu and Mbwekuru rivers are relatively small, mostly lying in the Masasi Spur (Fig. 1). The heavy mineral assemblages in samples from both rivers are strongly dominated by calcic amphibole. These amphiboles were likely derived from amphibolite facies rocks in the Masasi Spur (Kröner et al., 2003; Thomas et al., 2014; Mtabazi et al., 2019; Fossum et al., 2019). The comparable heavy mineral assemblages of the Matandu and Mbwekuru river samples indicate that both rivers carry sediments derived from similar lithotectonic units. In contrast, the zircon age distributions in the samples are distinctly different due to the high content of Palaeoproterozoic grains in the Matandu River sample, and the absence of those grains in the Mbwekuru River sample (Fig. 2). Thus, the isotopic zircon data

indicate that the Matandu River is draining an additional terrane not included in the Mbwekuru catchment area.

In all of the studied samples two common Neoproterozoic zircon age fractions were detected: 760–600 Ma (formed during the East African Orogeny) and 600–500 Ma (formed during the Kuunga Orogeny), and are most likely derived from the Mozambique Belt (Fig. 1). The Late Mesoproterozoic to Early Neoproterozoic age fraction (c. 1000 Ma) is probably derived from the Unango and Marrupa complexes in northern Mozambique and southern Tanzania (Fig. 1). The Palaeoproterozoic age fraction displays Usagaran ages of between 2000 and 1800 Ma. The detrital zircon population in the Mbwekuru River is more similar to the Ruvuma River, whereas the Matandu River displays similarities with the Rufiji River sample which also is characterised by a high content of Palaeoproterozoic grains. The majority of the concordant zircons in the Mbwekuru river sample display Kuunga ages (527–608 Ma), while the Late Mesoproterozoic age fraction, representing almost one third of the concordant zircons, displays ages typical of the Unango and Marrupa complexes. Scattered exposures of orthogneiss with protolith ages between 1100 and 900 Ma have been reported from the Masasi Spur and in the Mandawa Basin (Fig. 1). Consequently, the Late Mesoproterozoic to Early Neoproterozoic age fraction in the Matandu and Mbwekuru river samples is interpreted to be sourced from magmatic inliers of the Unango and Marrupa complexes in the Masasi Spur (Fig. 1). The Late Neoproterozoic – Cambrian age fraction is likely derived from granites emplaced during the end of the Kuunga Orogeny (Fig. 2). These rocks have been identified from the Mandawa Basin and the adjacent Masasi Spur (Thomas et al., 2014; Mtabazi et al., 2019). The concordant zircon population in the Ruvuma samples is strongly dominated by Late Mesoproterozoic to Early Neoproterozoic grains dated from 969 ± 10 to 1165 ± 10 Ma (Fig. 5), derived from the Unango and Marrupa complexes (Bingen et al., 2009). The smaller Neoproterozoic fraction might be derived from felsic plutons within the Unango and Marrupa complexes, and/or the Cabo Delgado Nappe Complex (Fig. 1).

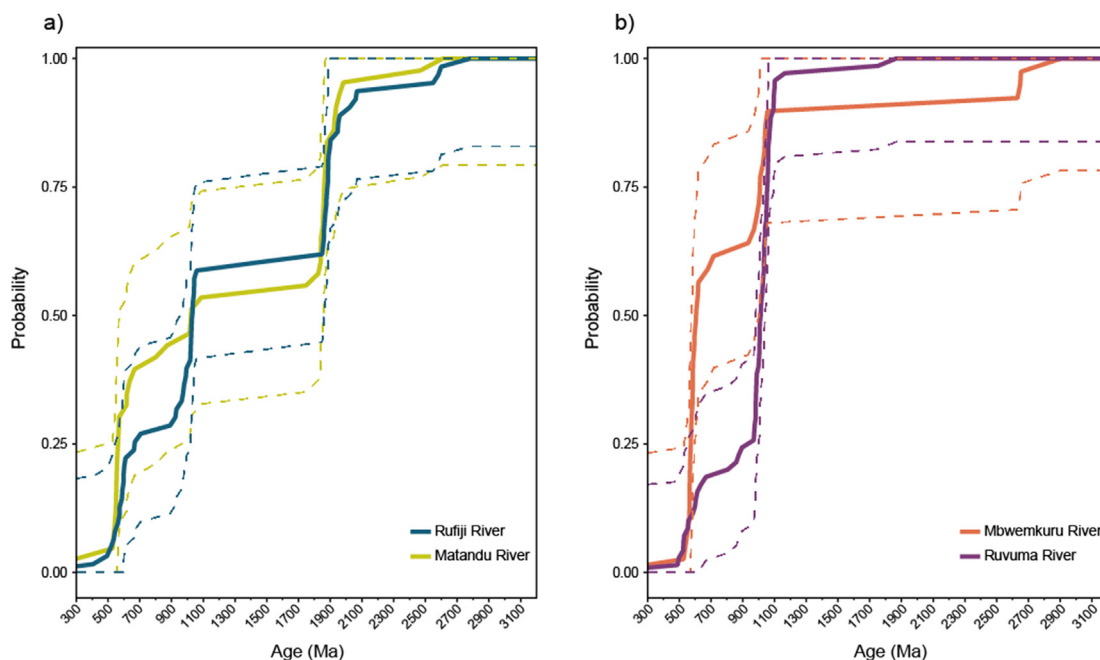


Fig. 6. Empirical cumulative distribution curves with the 95% confidence bands (broken lines) for the U/Pb zircon ages. a) The zircon age distribution is similar for the Rufiji River and the Matandu River samples, with overlapping confidence bands. b) The Mbwekuru River and Ruvuma River also display similar cumulative distribution curves with partly overlapping confidence bands.

The two most northerly rivers, the Rufiji and the Matandu, have similar zircon age distributions, both containing high amounts of Palaeoproterozoic grains (Fig. 5). The main difference in the zircon age distribution between the two river samples is the low contribution of Late Mesoproterozoic to Early Neoproterozoic zircons in the Matandu River (Fig. 5). The cumulative distribution curves of the zircon ages constructed for the Matandu and Rufiji river samples with overlapping 95% confidence bands, demonstrates the strong similarities between the zircon age distribution in the two data sets (Fig. 6). The zircon data illustrates that the Matandu River drains an additional terrane than the Mbemwemkuru River with abundant Palaeoproterozoic zircon grains. Because no Palaeoproterozoic rocks have been reported from the Masasi Spur, re-sedimentation of older sedimentary sequences which have acted as a repository for the Palaeoproterozoic zircons is a plausible explanation for their appearing in such abundances in the Matandu River. Most of the Matandu River catchment lies in the Masasi Spur, but the headwaters are in the Selous Basin (Fig. 1). The Selous Basin is the largest Karoo basin in Tanzania covering an area of 60,000 km². The bedrock is composed mainly of Upper Permian and Triassic successions with an estimated total thickness of 6000 m (Hankel, 1987). The Rufiji drains part of the Usagaran Belt, but the Matandu River does not (Fig. 1). The northeastern parts of the Selous Basin are drained partly by the Luwegu and Matandu rivers (Fig. 1). Given that this is the only area drained by both rivers it suggests that the Palaeoproterozoic zircons might be sourced from the Karoo rocks exposed in this part of the Selous Basin which has acted as a repository of these zircon grains. Unfortunately, no detrital zircon data have been reported from the Selous Basin. A sediment provenance analysis of the Permo–Triassic successions in the Karoo basins of SE Tanzania would shed light on the source-to-sink relationships in these intracratonic basins, and allow more precise interpretation of the data presented in this study.

4.2. Sink-to-source through time

Published provenance studies of Mesozoic and Cenozoic sandstones (Fossum et al., 2019) and Mesozoic siltstones (Caracciolo et al., 2019) in the Mandawa Basin allow us to compare the provenance signatures today with those of the past, and to detect if there has been any major change of source terranes from the Jurassic to present. However, comparing the heavy mineral signatures of the recent river sediments with that of e.g. Mesozoic sandstones is complicated because of the additional modifications during different sediment cycles, e.g. sorting during deposition, mineral dissolution during burial and recent weathering at outcrop (Johnsson, 1993; Morton and Hallsworth, 1994). As a result, sandstones would in most cases contain a more stable heavy mineral assemblage relative to recent river sediments, which often have a greater proportion of unstable heavy minerals as observed in this study.

The Jurassic to Paleogene sandstones in the Mandawa Basin were generally found to contain very similar heavy mineral assemblages dominated by garnets (Fossum et al., 2019). Single-grain analyses of the garnet and zircon populations from garnet-dominated heavy mineral assemblages concluded that the sediments were derived from multiple source terrains. This multi-source signature was interpreted to be a result of extensive sediment mixing during transport by a fluvial system which drained an extensive and heterogeneous catchment, similar to the Rufiji River today (Fossum et al., 2019). Thus, the Rufiji River is possibly a very old river system which history may extend back to the Middle – Late Jurassic times, similar to the modern Zambezi River where the lower and middle parts of the river follow Permo-Triassic Karoo rift valleys (Key et al., 2015).

Changes in sandstone composition, as a result of different provenance, are inferred to have taken place in the Early Cretaceous times; first in the Neocomian with deposition of amphibolitic sediments of the Nalwehe Formation, and later in the Aptian with the deposition of the Makonde Formation (Fossum et al., 2019). The amphibole-dominated

heavy mineral assemblage in the Neocomian sandstones is similar to the present heavy mineral assemblages in the Matandu and Mbemwemkuru river samples. The Aptian Makonde Formation was the only formation which contained a large contribution of Palaeoproterozoic detrital zircons and was characterised by a very stable heavy mineral assemblage strongly dominated by zircons. The Palaeoproterozoic zircons were interpreted to be derived from recycled Karoo successions based on the confined occurrence of sandstones carrying this provenance signal (Fossum et al., 2019). The same Palaeoproterozoic signature was also observed in Lower Cretaceous siltstones from another Mandawa Basin provenance study (Caracciolo et al., 2019). The appearance of abundant Palaeoproterozoic zircons in the Lower Cretaceous siltstones was interpreted to represent an Early Cretaceous broadening of the drainage system to include the Usagaran Belt (Caracciolo et al., 2019). However, in their study the analysed samples were not assigned to specific formations but rather grouped into Middle – Upper Jurassic and Lower Cretaceous successions. The majority of the samples categorised as Lower Cretaceous can be assigned to one of the Aptian – Albian formations including the Makonde Formation; the other samples are likely misplaced and should belong to the Jurassic when cross-referenced with the geological Mandawa Basin map of Hudson (2011).

The deposition of sediments enriched in Palaeoproterozoic zircons seems to have occurred in the Aptian which can be explained by exhumation and re-sedimentation of older sedimentary successions containing Palaeoproterozoic derived material, and does not necessarily indicate a widening of the drainage system. Fission track data from basement rocks in Tanzania suggest increased denudation rates during the Early Cretaceous, c. 140–120 Ma (Noble and Foster, 1997).

The common denominator, the Late Neoproterozoic to Cambrian and Late Mesoproterozoic to Early Neoproterozoic zircons, are the same as for zircons in the river sediments today. An additional zircon population, dated at c. 800 Ma, was also abundant in the Mandawa Basin sandstones. These 800 Ma zircons are rare in the recent river samples, with only a few grains detected in the Matandu and Ruvuma river samples (Fig. 5). This implies that 800 Ma terranes which were supplying abundant material in the past, are probably not supplying sediment now. This may be the result of complete erosion of these 800 Ma terranes, and/or re-organisation of the river tributaries into new catchment areas. The c. 800 Ma zircons were probably sourced from the Eastern Granulite e.g. the Mahange and Uluguru mountains (Fig. 1), where rocks with crystallisation ages between 880 and 739 Ma are reported (Fritz et al., 2005; Tenczer et al., 2006). Today, the Mahange Mountains are positioned within the Rufiji River Basin but the zircon data suggest that sediment contribution from these lithotectonic units is minimal.

The main reason for the different zircon age distribution in the Matandu and Rufiji river samples, and in the Ruvuma and Rufiji river samples (Figs. 5 and 6) is likely because the Matandu and Rufiji rivers also drain Karoo rocks (Fig. 1). Consequently, a significant part of the sediments supplied into the Indian Ocean by the Rufiji River today will comprise recycled sedimentary rocks.

More data are needed for more precise evaluation of the ancient source-to-sink and sedimentary transport systems. One of the main challenges in provenance studies such as this one is to recognise which grains are recycled and which grains are not. To identify the recycled material, similar studies of Karoo and other Mesozoic successions must be initiated. Sedimentary rocks have been, and still are, a major sediment supplier in south-central and coastal Tanzanian areas. It is important to recognise the recycled fingerprint in order to decipher the sink-to-source relationships and make better predictions on sediment dispersal through time.

5. Conclusions

- The heavy mineral assemblages in samples from the Matandu and Mbemwemkuru rivers were less diverse and dominated by more

unstable minerals dominated by calcic amphibole than samples from the larger Rufiji and Ruvuma rivers.

- The Ruvuma and Mbemkuru sediment samples contained two zircon age fractions derived from the Cabo Delgado Nappe Complex/Eastern Granulites and the Unango and Marrupa complexes.
- The abundant Palaeoproterozoic age fraction in the zircon populations in the Rufiji and Matandu river samples were interpreted as recycled grains from older Karoo successions in the Selous Basin.
- The high zircon diversity in the Rufiji River sample reflects a wide catchment area in which zircons were supplied from Karoo formations in addition to basement rocks. Similar zircon diversities in the Mesozoic sandstones of the Mandawa Basin suggest that an extensive fluvial system operated in SE Tanzania during the Jurassic.

As a final note, we want to highlight the advantages and possibilities for applying such provenance analytical methods to reservoir sandstones sampled from offshore wells. By using these simple methods, changes in sediment input can be recognised, and by mapping sand bodies with similar provenance signature one can determine sediment dispersal patterns and e.g. the extent of sand sheets. The heavy mineral data can also be applied for dating/correlation sections where the biostratigraphic control is poor.

Declaration of competing interest

All authors have approved this manuscript for submission to the Journal of African Earth Sciences. The authors have no conflicts of interest to declare. This study was funded by Equinor Tanzania (grant number 690354).

Acknowledgments

We would like to thank Equinor for funding this research through the Mandawa Basin Project. We also wish to thank Magnus Kristoffersen for assistance with the LA-ICP-MS, and to Nana Yaw Agyei-Dwarko for assistance with the U–Pb analyses, and Tom Andersen. Adrian Read and Bernard Bingen are thanked for improving the earlier versions of this paper.

Appendix A. Supplementary data

Supplementary data to this article can be found online at <https://doi.org/10.1016/j.jafrearsci.2020.103900>.

References

- Alizai, A., Carter, A., Clift, P.D., Van Laningham, S., Williams, J.C., Kumar, R., 2011. Sediment provenance, reworking and transport processes in the Indus River by U–Pb dating of detrital zircon grains. *Global Planet. Change* 76, 33–55.
- Andersen, T., Andersson, U.B., Graham, S., Åberg, G., Simonsen, S.L., 2009. Granitic magmatism by melting of juvenile continental crust: new constraints on the source of Palaeoproterozoic granitoids in Fennoscandia from Hf isotopes in zircon. *J. Geol. Soc.* 166, 233–247.
- Andersen, T., Elburg, M., Cawthorn-Balzeby, 2016. U–Pb and Lu–Hf zircon data in young sediments reflect sedimentary recycling in eastern South Africa. *J. Geol. Soc.* 173, 337–351.
- Andersen, T., Kristoffersen, M., Elburg, M.A., 2018. Visualizing, interpreting and comparing detrital zircon age and Hf isotope data in basin analysis – a graphical approach. *Basin Res.* 30, 132–147.
- Belousova, E.A., Griffin, W.L., O'Reilly, S.Y., 2006. Zircon crystal morphology, trace element signatures and Hf isotope composition as a tool for petrographic modelling: examples from eastern Australian granitoids. *J. Petrol.* 47, 329–353.
- Bingen, B., Jacobs, J., Viola, G., Henderson, I., Skår, Ø., Boyd, R., Thomas, R., Solli, A., Key, R., Daudi, E., 2009. Geochronology of the Precambrian crust in the Mozambique belt in NE Mozambique, and implications for Gondwana assembly. *Precambrian Res.* 170, 231–255.
- Boniface, N., Schenk, V., 2012. Neoproterozoic eclogites in the paleoproterozoic ubendian belt of Tanzania: evidence for a pan-African suture between the Bangweulu Block and the Tanzania craton. *Precambrian Res.* 208, 72–89.
- Bourget, J., Zaragosi, S., Garlan, T., Gabelotaud, I., Guyomard, P., Dennielou, B., Ellou-
- Zimmermann, N., Schneider, J.L., 2008. Discovery of a giant deep-sea valley in the Indian Ocean, off eastern Africa: the Tanzania channel. *Mar. Geol.* 255, 179–185.
- Caracciolo, L., Andò, S., Vermeesch, P., Garzanti, E., McCabe, R., Barbarano, M., Palcari, C., Rittner, M., Pearce, T., 2019. A multidisciplinary approach for the quantitative provenance analysis of siltstone. Mesozoic Mandawa Basin, southeastern Tanzania. In: In: Dowey, P., Osborne, P., Volk, H. (Eds.), *Application of Analytical Techniques to Petroleum Systems*, vol. 484. Geological Society, London, Special Publications, pp. 84–2018.
- Catuneanu, O., Wopfner, H., Eriksson, P.G., Cairncross, B., Rubidge, B.S., Smith, R.M.H., Hancox, P.J., 2005. The Karoo basins of south-central Africa. *J. Afr. Earth Sci.* 43, 21–253.
- De Waele, B., Kampunzu, A.B., Mapani, B.S.E., Tembo, F., 2006. The mesoproterozoic Irumide belt of Zambia. *J. Afr. Earth Sci.* 46, 36–70.
- Eagles, G., König, M., 2008. A model of plate kinematics in Gondwana breakup. *Geophys. J. Int.* 173 (2), 703–717.
- Fossum, K., Morton, A.C., Dypvik, H., Hudson, W.E., 2019. Integrated heavy mineral study of Jurassic to Paleogene sandstones in the Mandawa Basin, Tanzania: sediment provenance and source-to-sink relations. *J. Afr. Earth Sci.* 150, 546–565.
- Fritz, H., Tenczer, V., Hauzenberger, C.A., Wallbrecher, E., Hoinkes, G., Muhongo, S., Mogessie, A., 2005. Central Tanzanian tectonic map: a step forward to decipher Proterozoic structural events in the East African Orogen. *Tectonics* 24, TC6013.
- Fritz, H., Abdelsalam, M., Ali, K.A., Bingen, B., Collins, A.S., Fowler, A.R., Ghebream, W., Hauzenberger, C.A., Johnson, P.R., Kusky, T.M., Macey, P., Muhongo, S., Stern, R.J., Viola, G., 2013. Orogen styles in the East African orogen: a review of the neoproterozoic to cambrian tectonic evolution. *J. Afr. Earth Sci.* 86, 65–106.
- Gaina, C., Torsvik, T.H., van Hinsbergen, D.J., Medvedev, S., Werner, S.C., Labails, C., 2013. The African Plate: a history of oceanic crust accretion and subduction since the Jurassic. *Tectonophysics* 604, 4–25.
- Geiger, M., Clark, D.N., Mette, W., 2004. Reappraisal of the timing of the break-up of Gondwana based on sedimentological and seismic evidence from the Morondava Basin, SW Madagascar. *J. Afr. Earth Sci.* 338, 363–381.
- Haldemann, E.G., 1962. The Geology of the Rufiji Basin with Reference to Proposed Dam Sites. Government printer, Dar es Salaam, Tanzania, pp. 77pp.
- Hankel, O., 1987. Lithostratigraphic subdivision of the Karoo rocks in the Luwigo Basin (Tanzania) and their biostratigraphic classification based on microfloras, macrofloras, fossil wood and vertebrates. *Geol. Rundsch.* 76, 539–565.
- Hauzenberger, C.A., Tenczer, V., Bauernhofer, A., Fritz, H., Klötzli, U., Košler, J., Wallbrecher, E., Muhongo, S., et al., 2014. Precambrian Res. 255, 144–162.
- Hudson, W.E., 2011. The Geological Evolution of the Petroleum Prospective Mandawa Basin Southern Coastal Tanzania. Unpublished PhD Thesis. Trinity College, University of Dublin, Ireland, pp. 357.
- Huhma, H., Mänttari, I., Peltonen, P., Kontinen, A., Halkoaho, T., Hanski, E., Hokkanen, T., Hölttä, P., Juopperi, H., Konnunaho, J., Layahe, Y., Luukkonen, E., Pietikäinen, K., Pulkkinen, A., Sorjonen-Ward, P., Vaasjoki, M., Whitehouse, M., 2012. The Age of the Archaean Greenstone Belts in Finland. 54. pp. 74–175 Geological Survey of Finland, Special Paper.
- Johnsson, M.J., 1993. The System Controlling the Composition of Clastic Sediments. Geological Society of America, pp. 1–19 Special Paper 284.
- Kent, P.E., Hunt, J.A., Johnstone, D.W., 1971. The Geology and Geophysics of Coastal Tanzania. Natural Environment Research Council, Institute of Geological Sciences, pp. 101 Geophysical paper 6.
- Key, R.M., Cotterill, F.P.D., Moore, A.E., 2015. The Zambezi River: an archive of tectonic events linked to the amalgamation and disruption of Gondwana and subsequent evolution of the African plate. *S. Afr. J. Geol.* 118, 425–438.
- Kröner, A., Muhongo, S., Hegner, E., Wingate, M.T.D., 2003. Single-zircon geochronology and Nd isotopic systematics of Proterozoic high-grade rocks from the Mozambique belt of southern Tanzania (Masasi area): implications for Gondwana assembly. *J. Geol. Soc.* 160, 745–757.
- Macgregor, D., 2017. History of the development of Permian–Cretaceous rifts in East Africa: a series of interpreted maps through time. *Petrol. Geosci.* 24, 8–20.
- Malusa, M.G., Resentini, A., Garzanti, E., 2016. Hydraulic sorting and mineral fertility bias in detrital geochronology. *Gondwana Res.* 31, 1–19.
- Mbede, E.I., 1991. The sedimentary basins of Tanzania – reviewed. *J. Afr. Earth Sci.* 13, 291–387.
- Mbede, E.I., Dualeh, 1997. The coastal basins of Somalia, Kenya and Tanzania. In: Selly, R.C. (Ed.), *African Basins. Sedimentary Basins of the World*, pp. 211–233.
- Meert, J.G., 2003. A synopsis of events related to the assembly of Gondwana. *Tectonophysics* 362, 1–40.
- Mpanda, S., 1997. Geological Development of the East African Coastal Basin of Tanzania. PhD thesis. Department of Geology and Geochemistry, Stockholm University, Sweden, pp. 121.
- Mtabazi, E.G., Boniface, N., Andresen, A., 2019. Geochronological characterization of a transition zone between the Mozambique belt and Unango and Marrupa complexes complex in SE Tanzania. *Precambrian Res.* 321, 134–153.
- Morton, A.C., Hallsworth, C., 1994. Identifying provenance-specific features of detrital heavy mineral assemblages in sandstones. *Sediment. Geol.* 90, 241–256.
- Nicholas, C.J., Pearson, P.N., McMillan, I.K., Ditchfield, P.W., Singano, J.M., 2007. Structural evolution of southern coastal Tanzania since the Jurassic. *J. Afr. Earth Sci.* 48, 273–297.
- Noble, W., Foster, A., 1997. The post-Pan-African thermal and extensional history of crystalline basement rocks in Tanzania. *Tectonophysics* 275, 331–350.
- Pinna, P., Jourde, G., Calvez, J., Mroz, J., Marques, J., 1993. The Mozambique Belt in northern Mozambique: Neoproterozoic (1100–850 Ma) crustal growth and tectogenesis, and superimposed Pan-African (800–550 Ma) tectonism. *Precambrian Res.* 62, 1–59.
- Pinna, P., Muhongo, S., Le Goff, E., Mcharo, B.A., Deschamps, Y., Milesi, J.P., Vinauger,

- P., Ralay, F., 2004. Geology and Mineral Map of Tanzania Scale 1:2,000,000. Geological Survey of France, Orleans.
- Rabinowitz, P., Coffin, M., Falvey, D., 1982. Salt diapirs bordering the continental margin of northern Kenya and southern Somalia. *Science* 215, 663–665.
- Reeves, C.V., 2018. The development of the East African margin during Jurassic and Lower Cretaceous times: a perspective from global tectonics. *Petrol. Geosci.* 24, 41–56.
- Said, A., Moder, C., Clark, S., Abdelmalak, M.M., 2015. Sedimentary budgets of the Tanzania coastal basins and implications for uplift history of the East African rift system. *J. Afr. Earth Sci.* 111, 288–295.
- Sommer, Kröner, A., Lowry, J., et al., 2017. Neoproterozoic eclogite-to high-pressure granulite-facies metamorphism in the Mozambique belt of east-central Tanzania: A petrological, geochemical and geochronological approach. *Lithos* 284, 666–690.
- Steiger, R., Jäger, E., 1977. Subcommission on geochronology: convention on the use of decay constants in geo- and cosmochronology. *Earth Planet Sci. Lett.* 36, 359–362.
- Temple, P.H., Sundborg, Å., 1972. The Rufiji River, Tanzania hydrology and sediment transport. *Geogr. Ann. Phys. Geogr.* 54, 345–368.
- Torsvik, T.H., Cocks, L.R., 2013. Gondwana from top to base in space and time. *Gondwana Res.* 24, 999–1030.
- Tenczer, V., Hauenberger, C., Fritz, H., Whitehouse, M., Mogessie, A., Wallbrecher, E., Muhongo, S., Hoinkes, G., 2006. Anorthosites in the Eastern Granulites of Tanzania—new SIMS zircon U–Pb age data, petrography and geochemistry. *Precambrian Res.* 148, 85–114.
- Thomas, R.J., Bushi, A.M., Roberts, N.M., Jacobs, J., 2014. Geochronology of granitic rocks from the Ruangwa region, southern Tanzania—Links with NE Mozambique and beyond. *J. Afr. Earth Sci.* 100, 70–80.
- Tuck-Martin, A., Adam, J., Eagles, G., 2018. New plate kinematic model and tectono-stratigraphic history of the East African and west madagascan margins. *Basin Res.* 30, 1118–1140.
- Van der Beek, P., Mbede, E., Andriessen, P., Delvaux, D., 1998. Denudation history of the Malawi and Rukwa rift flanks (East African Rift System) from apatite fission track geochronology. *J. African Earth Sci.* 26, 363–385.
- Wiedenbeck, M., Allé, P., Corfu, F., Griffin, W.L., Meier, M., Oberli, F., Von Quadt, A., Roddick, J.C., Spiegel, W., 1995. Three natural zircon standards for U-Th-Pb, Lu-Hf, trace element and REE analysis. *Geostand. Newsl.* 1–23.
- Wopfner, H., 2002. Tectonic and climatic events controlling deposition in Tanzanian Karoo basins. *J. Afr. Earth Sci.* 34, 167.